# DEVELOPMENT OF INSERTION DEVICE MAGNETIC CHARACTERIZATION SYSTEMS AT LNLS

G. Tosin, J.F. Citadini, R. Basílio and M. Potye, LNLS, Campinas, Brazil.

*Abstract*

This paper describes a set of magnetic measurement systems employed in the development of insertion devices at LNLS (Brazilian Synchrotron Light Source). They are: rotating coil (which can also operate as a flip-coil), spatial field mapping using Hall probes and parallel coils (Helmholtz configuration) for magnetic blocks characterization. Although such techniques are well established, strict specifications imposed by the beam dynamics on the magnetic field quality, led to a detailed analysis of the sources of error and their minimization. All three systems have already been tested and showed excellent accuracy and repeatability when compared to typical values found in the scientific literature.

## INTRODUCTION

Three systems dedicated to insertion device (ID) magnetic characterization were built and tested. They are: rotating coil for integrated field measurements, Hall probes bench for local field determination and two parallel coils for discovering the blocks' magnetic moments. Some particular features were introduced to improve both accuracy and repeatability. Rotating coil and Hall probes performance were checked by measuring a 2 T hybrid wiggler having 2.8 meters in length. Two parallel coils system was tested by characterizing the blocks of the elliptically polarized undulator under construction.

## ROTATING COIL

Figure 1 is a schematic drawing showing all parts of the rotating coil experimental arrangement. The coil is composed of 25 turns of tungsten wires, stretched with a total force of 85 kgf by means of springs. Figure 2 illustrates how the wires were wound in the reference guides to avoid the formation of coil imperfections (bumps in the wires). Such design does not allow one turn to touch the others. Parker drivers control the motors for rotational and linear translation movements. The drivers for rotational movement are connected in parallel, having the same address, to assure the motors a matching behavior. The coil angular position is obtained by A and B rotational encoders, while A and B linear encoders are used for transversal displacement reading. The induced voltage in the coil is amplified and delivered to the Metrolab integrator PDI5025, this detection being synchronized with the rotational encoder pulses. The data are computationally treated. Main operation parameters are listed in Table 1.

Many sources of errors were exhaustively studied: coil imperfections (local bumps), reference guides of opposite coil extremities with different diameters, gravitational sag, centripetal deformation, central coil leg displaced from rotating center, ID not centralized in the coil, vibrations, temperature variation, external electromagnetic noise, conductor wire position in the coil, angular torsion and angular offset, coil area size, changes of the electric offset during one coil turn and electrical noises.

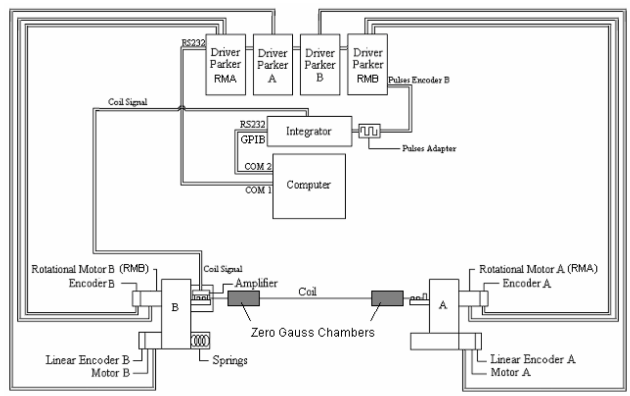


Figure 1: Schematic drawing of rotating coil system

Coil imperfections are the most significant sources of errors, which effect can hide completely the true value of the integrated field. To evaluate this error magnitude, the ID should be longitudinally displaced by the overall distance of one magnetic period or more. Plotting the integrated field as a function of the displacement, a periodic behavior having the same field periodicity is observed. This oscillation amplitude corresponds to the maximum disturbance that this source of error introduces on the measurement.

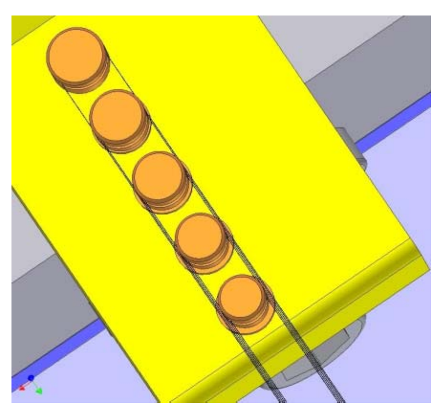

Figure 2: Turns assembly to reduce imperfections in the coil extent

In order to observe the distribution of imperfections along the coil, a dipolar localized field is placed in several sequential positions and for each position the dipolar components are measured. The dipolar component measured is proportional to main radius in the region where the dipole is placed, obtaining in such way the coil radius variation as a function of the longitudinal coil part.

Table 1: Rotating coil main parameters

| | |
|---|---|
| Length [m] | 4.2 |
| Number of turns | 25 |
| Radius [mm] | 8.95 |
| Coil sides [mm] | 1.2 x 1.2 |
| Bare wire diameter [mm] | 0.1 |
| Insulated wire diameter [mm] | 0.15 |
| Coil sag [mm] | 0.25 |
| Electrical Resistance [Ω] | 1700 |
| Total strength applied on the coil [kgf] | 85 |
| Measurement angular speed [turns/s] | 1.6 |
| Acceleration [turn/$s^2$] | 21 |
| Number of acquisition per turn | 128 |
| Angular control [ $^0$] | 0.17 |

In order to achieve accuracy for far distances from the central line of the ID, the rotating coil operates as a flip-coil. In this case, the coil is transversely displaced, and for each position, only the dipolar components of the rotating coil are taken. A polynomial fit on the dipolar values as a function of the transverse displacement reveals the magnetic field multipolar composition.

The performance was tested in the 2 T wiggler and the results showed accuracy in the order of **$5\times10^{-6}$ T.m** and repeatability of **$\pm3\times10^{-7}$ T.m**, for the integrated field (dipolar component) in the worst case (minimum wiggler gap). The repeatability is the standard deviation of tens of measurements and the accuracy is estimated by means of three processes: error analysis, measurement of a well determined magnetic field and by the comparison with the results of the Hall probe bench.

Detailed explanations about all the topics mentioned in this section can be found in the references [1, 2].

## HALL PROBES

Three Sentron Hall probes (model YM12-3-2-2T), having their sensitive surfaces orthogonally oriented, were employed for local field measurement. This kind of probe was chosen for the followings reasons: small sensitive volume, no planar Hall effect, good linearity, good thermal stability and low electrical noise.

Figure 3 aids in the understanding of this brief description of the system operation: At the beginning of each scan, the probes are placed in a given (X, Z) transverse position and the scan occurs in Y direction. Three linear encoders read the probe position, however, only the Y encoder is read during the scan. Two zero Gauss chambers are placed at the extremities of the scan range to determine the voltage offset and its variation during the scan. External triggers for field measurements are provided by a pulse divisor, which generates one pulse for every set of pulses received from the rotational encoder. This pulse divisor can be selected from 1 to 256, to convert a carriage with the selected number of encoder pulses in only one trigger, changing the distance between successive points. This trigger enables simultaneously the voltmeter and the Y linear encoder readings. Voltage data are stored in the voltmeter memory while data from Y linear encoder are read directly by a micro computer. At the end of the scan, both data are merged in one file.

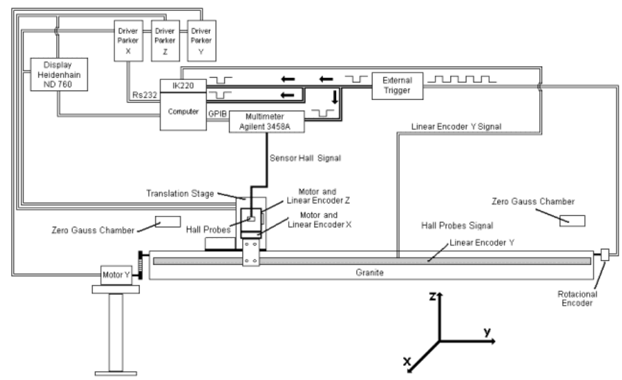


Figure 3: Set of equipment used for 3-Hall-probe scans

Table 2 contains the main parameters of the Hall probe bench system.

Table 2: Hall bench main parameters

| | |
|---|---|
| Total scan length (mm) | 4200 |
| Maximum n$^o$ of points per scan | 15200 |
| Smaller scan gap (mm) | 0.28 |
| Maximum speed (mm/s) | 75 |
| Voltmeter integration time (ms) | 0.167 |
| Linear encoders resolution (μm) | 0.1 |
| Linear encoders accuracy (μm) | ± 5 |
| Maximum angular probe error ( $^0$ ) | ± 0.5 |

The following random and systematic sources of errors were analyzed: electrical noises, variation in the probes speed, temperature variation (effect of the temperature on the magnetic field, on electronic equipments and on the Hall probe mechanical supports), electronic offset, accuracy of the zero Gauss chamber, angular probe misalignment, probe position (transverse probe displacements - X and Z axes, longitudinal probe displacements - Y axis, linear encoder errors and vibrations), eddy currents in Hall probe supports and probe calibration. The perception and reduction of the errors were essential to achieve high accuracy and precision.

The local field repeatability is the standard deviation of the measured field in a given position, considering tens of scans. The higher deviations were at maximum gradient regions, being attributed to the mechanical vibrations. They reached **$\pm$ 7 $\times$ $10^{-4}$ T** for the wiggler minimum gap, in a gradient of 66 T/m. In the regions of 2 T constant fields, the standard deviation was **$\pm$ 2 $\times$ $10^{-5}$**

**T**. For the maximum gap, 300 mm, the error was constant along the entire scan: ± **7 × 10$^{-6}$ T**. This value is in the same level of the electrical noise. The local field accuracy depends on the calibration table given by the manufacturer. The repeatability of the integrated field showed to be dependent on the wiggler gap. Hundreds of scans were made, presenting a standard deviation of **± 6.5 × 10$^{-6}$ × $B_p$ T.m**, where $B_p$ is the peak field in tesla (T). This expression is not valid for the larger gaps, in which the repeatability is **± 6 × 10$^{-7}$ T.m**. An indicative of the accuracy can be obtained comparing Hall bench results to the rotating coil measurements, since both were developed and worked in completely independent ways. An agreement in the order of **1 × 10$^{-5}$ T.m** was verified.

Reference [3] contains a better description of the hall bench above mentioned.

## TWO PARALLEL COILS

Figure 4 shows the equipment employed for the magnetic block characterization. The microcomputer controls the motor to set in motion the block by means of a Parker driver. A rotational encoder is attached to the motor shaft giving the angular position of the block. The induced signal in the coil is detected by the Metrolab voltage integrator PDI5025 and internally stored. The data are transferred to the microcomputer and the magnetic moments are calculated.

The blocks used for LNLS Insertion Devices have there main magnetization always perpendicular or parallel to their faces. The magnetization vector is measured in two stages: First, the main component is measured by installing the block inside the reference support (holder) in such a way to have this component pointing parallel to the normal coil surface vector. The block stability during the movement is guaranteed by one side screw. Afterwards, the residual components are determined by the positioning the block with its main component now in the vertical direction. This procedure allows the increasing of the voltage detection gain, improving its sensitivity. It also avoids the error arising from the main component projection on the residual components, when there is an angular encoder offset relative to the coil surfaces.

Table 3 summarizes the main characteristics of the block characterization system. Some of them are very similar to that presented in reference [4].

For every measurement the block is taken off and incased again in the holder. The magnetization units are written in terms of $\mu_o M$, which is typically 1.25 T for the LNLS magnets, being $\mu_o$ the magnetic permeability and M the magnetization. The angles α and β are defined as:

$$\alpha = arctan\left(\frac{m_x}{m_z}\right) \quad \text{and} \quad \beta = arctan\left(\frac{m_y}{m_z}\right)$$

where $m_z$ is the main component and $m_x$ and $m_y$ are the residuals components. Room temperature was held within 24 ± 0.4 $^0$C. Typical values for modulus repeatability (standard deviation) in a short time (10 successive acquisitions) is **7 × 10$^{-5}$ T** and for long time acquisitions (done during several days) is **7 × 10$^{-4}$ T**. α and β angles repeatability is smaller than **0.01$^0$**. The temperature of each block is measured and its magnetization is corrected by the factor of 1/1100 per $^0$C.

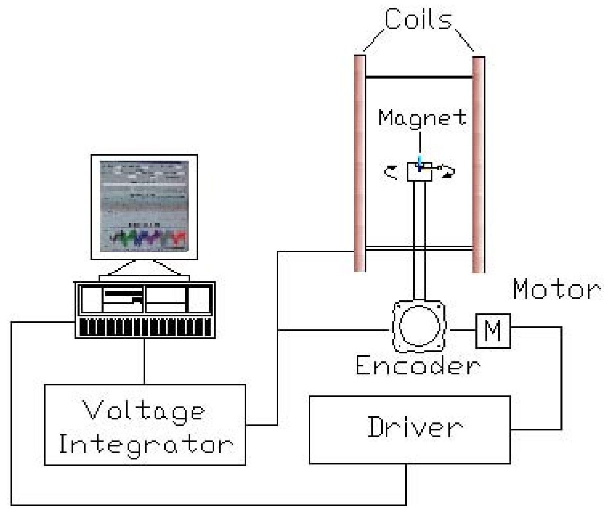


Figure 4: Schematic representation of the magnetic blocks characterization system

Table 3: Main parameters list

| | |
|---|---|
| Coil radius [mm] | 347.4 |
| Distance between the coils [mm] | 330.6 |
| Copper wire diameter [mm] | 0.25 |
| Coil transverse section [mm$^2$] | 22 x 6 |
| N$^o$ of turns/ coil | 1141 |
| Electrical resistance/ coil [Ω] | 854 |
| Angular speed [turns/s] | 1 |
| Alignment angular errors [degrees] | 0.1 |
| Position errors [mm] | 0.05 |
| Spent time for block [s] | 120 |

## REFERENCES

[1] G. Tosin, J.F. Citadini and E. Conforti, Long rotating coil system based on stretched tungsten wires for insertion devices characterization, IEEE Trans. Instrum. Meas., submitted for publication, 2005.

[2] G. Tosin, J.F. Citadini and E. Conforti, Long rotating coil system supported by “twaron” wires for insertion devices characterization. In: SBMO/IEEE MTT-S International Microwave and Optoelectronics Conference, 2005.

[3] G. Tosin; J.F. Citadini and E. Conforti, Hall Probe Bench for Insertion Devices Characterization at LNLS. IEEE Trans. Instrum. Meas., submitted for publication, 2005.

[4] C.S. Hwang, Shuting Yeh, P.K. Teng and T.M. Uen, Rev. Sci. Instrum. 67 (5), pp 1741-1747, 1996.